Supporting Information

A dexamethasone-eluting porous scaffold for bone regeneration fabricated by selective laser sintering

Zhidong Sun [a, b, h, 1], Fan Wu [c, d, 1], Huichang Gao [f], Kai Cui [a, b], Mengyue Xian [a, b], Jianglong Zhong [d], Ye Tian [g], Song Fan [c, d, **], Gang Wu [a, b, e, *]

[a] School of Materials Science and Engineering, South China University of Technology, Guangzhou, 510641, China

[b] National Engineering Research Center for Tissue Restoration and Reconstruction, South China University of Technology, Guangzhou 510006, P. R. China

[c] Guangdong Provincial Key Laboratory of Malignant Tumor Epigenetics and Gene Regulation of Sun Yat-Sen Memorial Hospital, Guangzhou 510120, China

[d] Department of Oral and Maxillofacial Surgery, Sun Yat-Sen Memorial Hospital of Sun Yat-Sen University, Guangzhou 510120, China

[e] Key Laboratory of Biomedical Engineering of Guangdong Province, South China University of Technology, Guangzhou 510006, P. R. China

[f] School of Medicine, South China University of Technology, Guangzhou 510006, P. R. China

[g] Department of medical devices, Guangdong food and Drug Vocational College, Guangzhou 510520, P. R. China

[h] Guangzhou Research Institute of Well Lead Medical Equipment Co., Ltd., Guangzhou 511434, P. R. China

* Corresponding author. School of Materials Science and Engineering, South China University of Technology, Guangzhou, 510641, China

E-mail: imwugang@scut.edu.cn

** Corresponding author. Guangdong Provincial Key Laboratory of Malignant Tumor Epigenetics and Gene Regulation of Sun Yat-Sen Memorial Hospital, Guangzhou 510120, China

E-Mail: fansong2@mail.sysu.edu.cn

[1] These authors are co-first authors and contributed equally to this work.

Experimental methods supplement

1. Develop a laser cutting machine into a selective laser sintering machine

The selective laser sintering machine used in this work is modified from a laser cutting machine (Dongguan Gbos Laser Technology Co., Ltd, China. Figure S1a). The modification process is shown in Figure S1. Briefly, the working platform, screen cloth and the exhaust pipe under the screen were removed, as shown in Figure S1a and b, then a round hole at the bottom was exposed. Subsequently, a self-designed and assembled printing platform device was introduced into the working area under the laser head through the round hole (Figure S1c). The printing platform device was composed of an retort stand, two attaching clamps, a micrometer caliper and a syringe (Figure S1d, e, f). The head of the syringe was flattened to fill the powder to be printed to form a printing platform (Figure S1e). The plunger of the syringe could be driven downward thought the micrometer caliper, as a result, the printing platform was lowered, then the powder supply was finished manually. It is worth mentioning that the minimum graduation value of the micrometer caliper is 20 μm, which is able to achieve a layer thickness of 100-200 μm (Figure S1g).

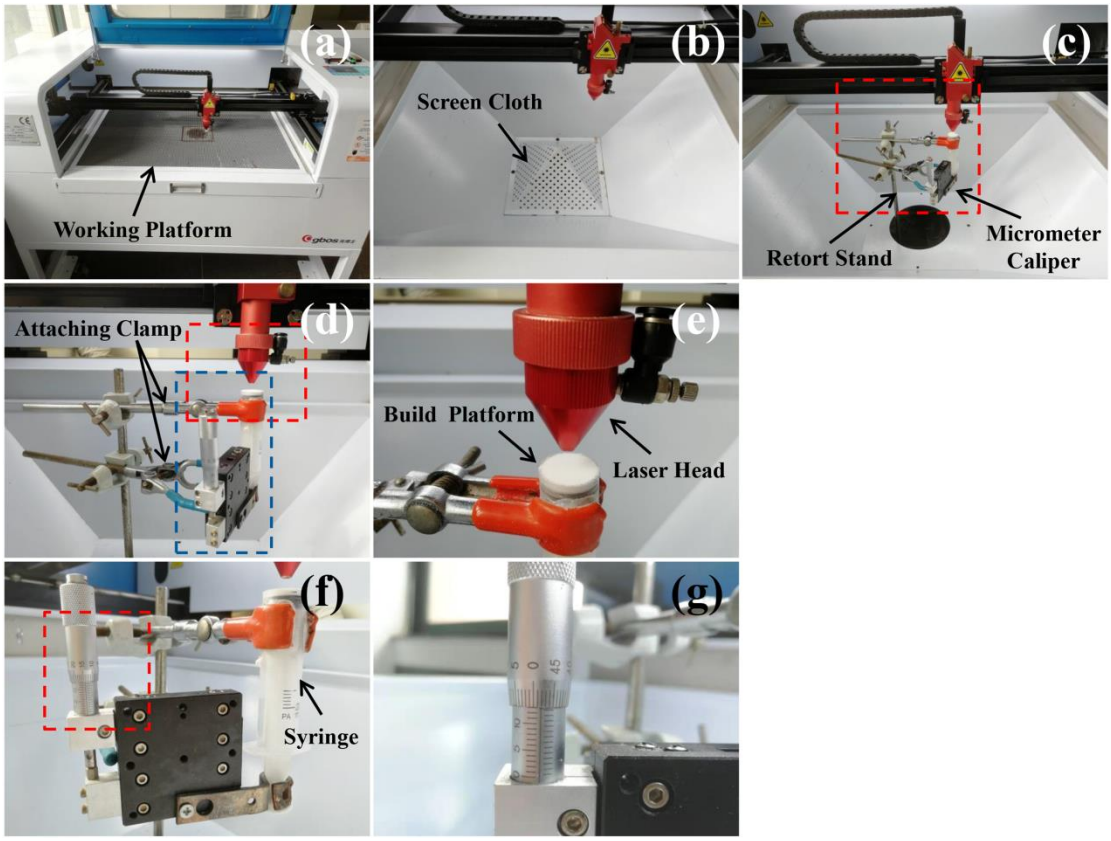

Figure S1. The modification process of developing a laser cutting machine into a selective laser sintering machine. (a) The laser cutting machine. (b) The laser cutting machine after removing the working platform. (c) The selective laser sintering machine modified from the laser cutting machine. (d) Enlarged image of the red dotted frame in (c). (e) Enlarged image of the red dotted frame in (d). (f) Enlarged image of the blue dotted frame in (d). (g) Enlarged image of the red dotted frame in (f).

2. FDM melting process to process PD microspheres

In order to compare the effects of FDM and SLS processing on the drug activity of

drug-loaded microspheres, a PD melt obtained by simulating the melting process of FDM was prepared. The PD microspheres were fused using a high temperature tube furnace (MXG1200-200, MICRO-X). The FDM printing temperature of polylactic acid is 190-230 ℃. It is estimated that it takes 15 minutes to print the scaffold shown in Figure 2 with FDM. Therefore, the working procedure of the high temperature tube furnace was set to be heated to 230 ℃ at a increasing rate of 5 ℃/min for 15 minutes under a nitrogen atmosphere, and then naturally cooled under the action of the nitrogen gas flow.

3. Mechanical tests

The mechanical properties of the scaffold samples were measured by a universal mechanical testing machine (INSTRON 5967). The loading rate is set at 1 mm/min. Each group contains five samples for repeated experiments, from which the mean and standard deviation are calculated.

4. Degradation in vitro

The degradation rate of the scaffolds was evaluated in PBS solution (pH=7.4) at 37 °C with the solid/liquid ratio of 10 mg/ml. The PBS solution was changed every week during the tests. The original weight (M_0) and the weight (M_1) at specific time points (3, 7, 14, 21 and 28 days) were collected after the sample was dried to constant weight. The weight loss rate was obtained by the following formula:

$$\text{Weight loss (\%)} = \frac{M_0 - M_1}{M_0} \times 100\%$$

Results supplement

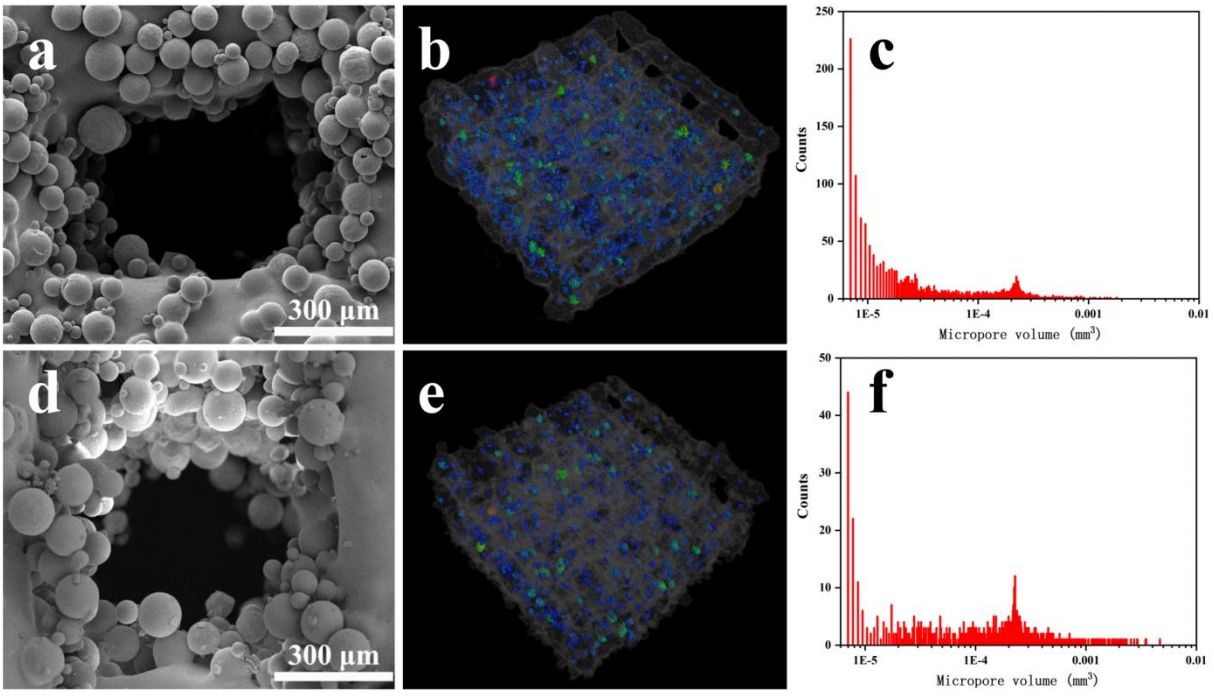

Figure S2. Distribution of microspheres and micropores in the scaffolds. SEM images of PLLA (a) and PB (d) scaffold with 160× magnification. Micropore distribution of PLLA (b) and PB (e) scaffold. Micropore volume distribution of PLLA (c) and PB (f) scaffold.

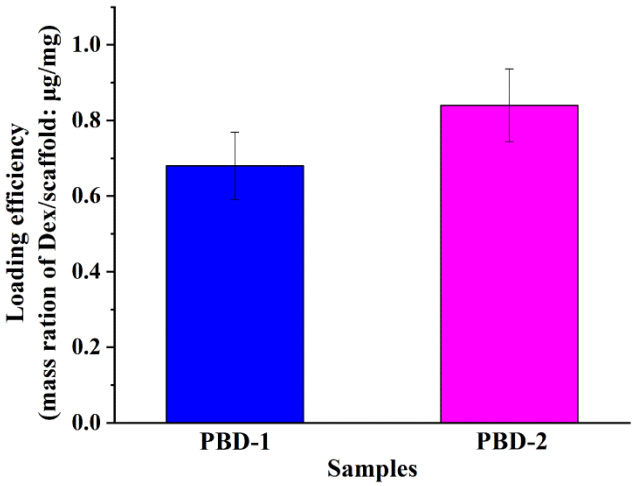

Figure S3. Drug loading efficiency of PBD-1 and PBD-2 scaffold.

The compressive stress-strain curves of various scaffolds were presented in Fig. S4a. For the composite scaffolds with various dexamethasone amount, the compression strength was within 1.3-1.5 MPa and the compression modulus was within 18-25 MPa. In contrast, the maximum compression strength and compression modulus of PLLA scaffold were only 0.9 MPa and 9.1 MPa respectively (Fig. S4b, c), indicating BG and dexamethasone added in microspheres significantly increased the scaffold mechanical properties.

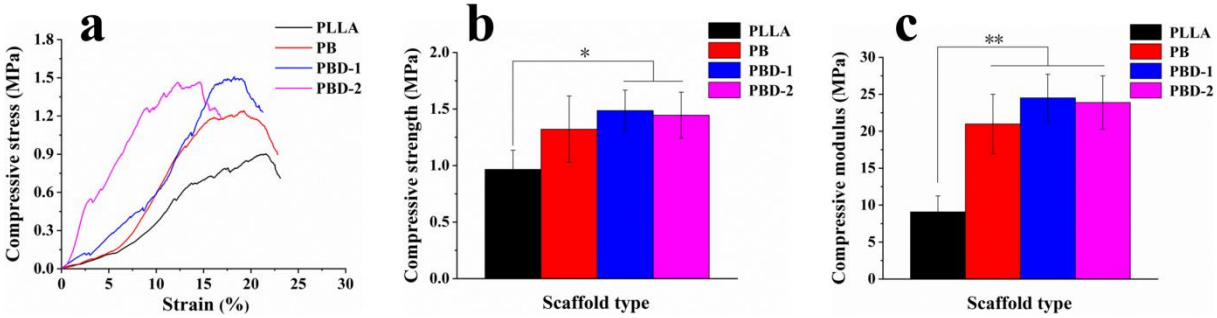

Figure S4. Mechanical properties of the scaffolds. (a) The curve of compressive strength with increasing scaffold deformation during compression testing for different type of samples. Compressive strength (b) and compressive modulus (c) of various scaffolds. **: $P < 0.01$. *: $0.01 < P < 0.05$.

Weight loss of the scaffolds along with time in PBS was shown in Fig. S5. All the scaffolds weight decreased with the increase of time. Compared with pure PLLA scaffold, all composite scaffolds showed slower weight loss during the first 7 days, but quicker weight reduction after that.

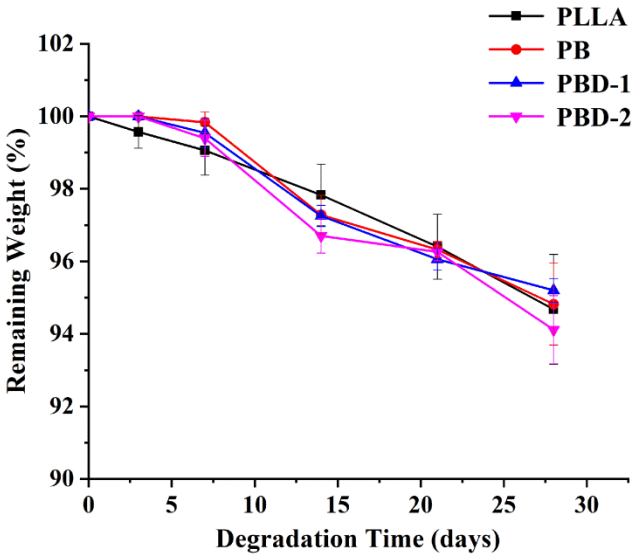

Figure S5. The change of weight loss of different scaffolds immersed in PBS solution with time.

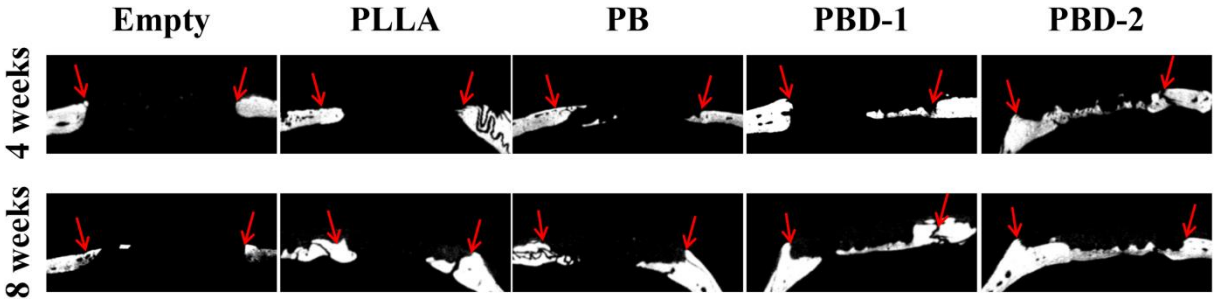

Figure S6. Micro-CT reconstruction images of the sagittal plane of rat crania at 4 and 8 weeks post-surgery. The red arrows in the figure indicate the location of the defect.

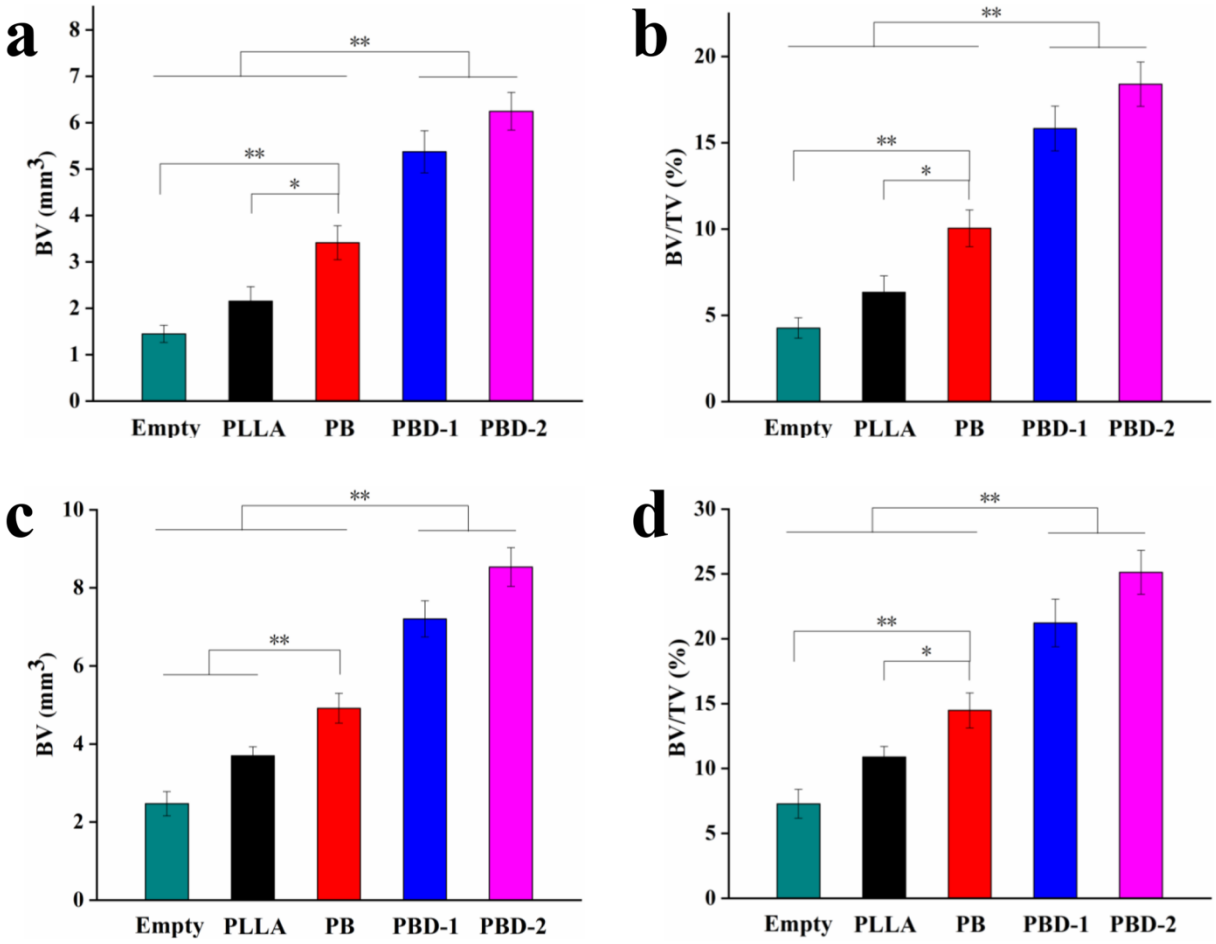

Figure S7. The new bone volume and new bone volume fraction of different samples. (a) (b) 4 weeks post-surgery. (c) (d) 8 weeks post-surgery. **: $P < 0.01$. *: $0.01 < P < 0.05$.